



Drought and deluge: the recurrence of hydroclimate extremes during the past 600 years in eastern Australia's Natural Resource Management (NRM) clusters

Jonathan G. Palmer^{1,2}  · Danielle Verdon-Kidd³ · Kathryn J. Allen^{1,4} · Philippa Higgins¹ · Benjamin I. Cook^{5,6} · Edward R. Cook⁵ · Christian S. M. Turney^{1,2,7} · Patrick J. Baker⁸

Received: 7 May 2023 / Accepted: 26 October 2023 / Published online: 12 December 2023
© The Author(s) 2024, corrected publication 2023

Abstract

Recent extremes of flood and drought across Australia have raised questions about the recurrence of such rare events and highlighted the importance of understanding multi-decadal climate variability. However, instrumental records over the past century are too short to adequately characterise climate variability on multi-decadal and longer timescales or robustly determine extreme event frequencies and their duration. Palaeoclimate reconstructions can provide much-needed information to help address this problem. Here, we use the 600-year hydroclimate record captured in the eastern Australian and New Zealand Drought Atlas (ANZDA) to analyse drought and pluvial frequency trends for East Australian Natural Resource Management (NRM) clusters. This partitioning of the drought atlas grid points into recognised biophysical areas (i.e. NRM clusters) revealed their differences and similarities in drought intensity and pluvial events over time. We find sustained multi-decadal periods of a wet–dry geographic ‘seesaw’ between eastern to central and southern NRMs (e.g. 1550–1600 CE and 1700–1750 CE). In contrast, other periods reveal spatially consistent wetting (e.g. 1500–1550 CE) or drying (e.g. 1750–1800 CE). Emerging hot spot analysis further shows that some areas that appear naturally buffered from severe drought during the instrumental period have a greater exposure risk when the longer 600-year record is considered. These findings are particularly relevant to management plans when dealing with the impacts of climate extremes developed at regional scales. Our results demonstrate that integrating and extending instrumental records with palaeoclimate datasets will become increasingly important for developing robust and locally specific extreme event frequency information for managing water resources.

Keywords Australian hydroclimate · Extreme event recurrence · Refugia · Temporal stability

1 Introduction

Future adaptation planning relies on understanding the environmental impacts of anthropogenic climate change and an appreciation of natural climate variability. While there is a high degree of certainty around the impacts of climate change on temperature, there has been less confidence in the hydroclimatic effects (IPCC 2021). Climate change is thought to have already accelerated the hydrological processes making droughts more severe on a global scale (Mukherjee et al. 2018); however, regional-scale processes, forcings and feedback can modulate the local expression of drought (Cook et al. 2022; Vogel et al. 2019). A further complication is the combination of relatively high variability and short instrumental records that do not adequately capture inherent natural variability and are unlikely to represent the full range of possible wet and dry extremes (Cook et al. 2022)—even without anthropogenically forced climate change. Included within these are a special category of extreme events that are relatively rare, have significant impacts and are of uncertain timing—sometimes described as Black Swans (Taleb 2007)—the lack of a suitable hydroclimate baseline makes it challenging to contextualise recent extremes and plan for the frequency and intensity of climate extremes.

Australia has one of the most variable hydroclimates in the world (Peel et al. 2004) and has experienced three major widespread and protracted droughts in the past 120 years (Verdon-Kidd and Kiem 2009). Over the past two decades alone, parts of Australia have experienced several significant pluvial events (e.g. 2011, 2019 and 2022 CE in Queensland) as well as persistent drought conditions (e.g. 2001–2009 and 2017–2019 CE in Southeast Australia). The estimated economic impact of the 2017–2019 CE drought and subsequent 2019–2020 CE bushfires was A\$63 billion (Wittwer and Waschik 2021). A lack of understanding of how unusual such events are presents an obstacle to effective adaptive planning. Extremes are infrequent by definition, meaning that the short instrumental hydroclimate record (e.g. rainfall and river flow) only contains a few samples of extreme wet and dry events. This creates significant challenges for generating probabilistic estimates of return periods: each time a new extreme occurs (e.g. a high rainfall event), the distribution is updated and event probabilities recalculated. A much longer context, as well as a larger pool of extreme events, are needed to robustly fit probability distributions. This would allow us to define better just how unusual recent events (often considered extreme) are against a long-term context, providing the data required for robust decision-making. Three examples include water allocation decision-making (e.g. Higgins et al. 2022), town planning decisions or identifying areas that can act as refugia for flora and fauna from extreme drought events.

Characterising the recurrence frequency of extreme events is helpful to land managers and planners but requires records with a precisely dated annual (or finer) resolution. Palaeoclimate reconstructions from tree rings may be especially useful in this regard because they provide a precisely dated and annually resolved record, normally over hundreds of years, with a resolution commensurate with that required for planning purposes. In particular, the eastern Australia and New Zealand Drought Atlas (ANZDA; Cook et al. 2016, 2018; Palmer et al. 2015) provides an annually-resolved gridded dataset of the Palmer Drought Severity Index (scPDSI) showing drought and pluvial periods across eastern Australia (Longitude > 136° E) over the past 600 years based on tree ring and coral chronologies. Such a record is especially valuable as the area covered includes large expanses of land under intensive agricultural use and most of eastern Australia's major population centres. The ANZDA is particularly useful in terms of identifying the broader spatial patterns

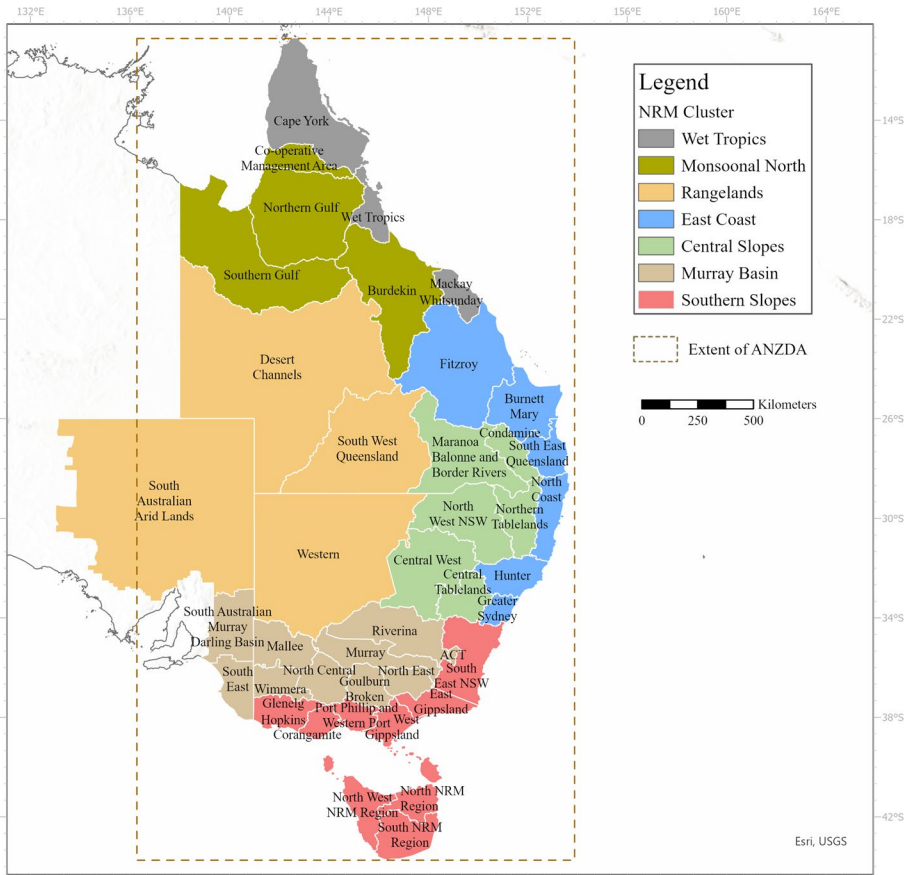


Fig. 1 Map of eastern Australia overlaid with the natural resource management (NRM) clusters coinciding within the eastern Australia Drought Atlas (orange box). Particular NRM areas contributing to the clusters are also indicated

in droughts and pluvials and, as such, matches the scale of information relevant to planners, resource and land managers.

In the Australian context, government agencies and non-government organisations utilise the 54 Natural Resource Management regions (NRMs) as a focus for national priorities in relation to environmental management and planning. These NRMs are often grouped into eight areas for broad-scale climate change studies based on climatic and biophysical information (CSIRO and Bureau of Meteorology 2015). As a result, each of the eight larger areas contains several NRMs and are generally described as ‘NRM clusters’—the Wet Tropics (WT), Monsoonal North (MN), Rangelands (RL), East Coast (EC), Central Slopes (CS), Murray Basin (MB) and Southern Slopes (SS). This regionality and the fact that climate projections for these NRM clusters exist (see: www.climatechangeinaustralia.gov.au) makes them an ideal target for examining regional natural hydroclimate variability over longer time frames (Freund et al. 2017; Grose et al. 2020). Here, we use the ANZDA resource to extract 600 years of hydroclimatic information for seven of the eight NRM clusters in eastern Australia (Fig. 1). We use this data to address whether the extent,

frequency, intensity and duration of droughts and pluvials experienced in recent decades will be sufficient to help us plan for the future (i.e. is this a good representation of baseline variability). Specifically, has the recurrence of droughts and pluvials changed over the past 600 years and is the current pattern of hydroclimate extremes in the different NRM clusters unusual in the context of the past ~600 years? We also illustrate how this type of information can reveal potential climate refugia or identify areas currently being considered as refugia that may, in fact, be vulnerable.

2 Data and methods

2.1 The eastern Australia and New Zealand Drought Atlas (ANZDA)

The ANZDA (Palmer et al. 2015) consists of a gridded (0.5° spatial resolution) network of annually resolved values of the self-calibrating Palmer Drought Severity Index (scPDSI; Palmer 1965; van der Schrier et al. 2013). The yearly values are for the austral summer (December, January and February), with positive scPDSI values indicating wetter than normal conditions, while negative values indicate drier than normal conditions (droughts). The drought index is a widely used palaeoclimate reconstruction target, especially by the well-known series of drought atlases derived from tree-ring networks (e.g. Cook et al. 2010, 2015, 2020; Cook 1999; Morales et al. 2020; Stahle et al. 2016), many of which have been collated into one portal for easier access (Burnette 2021). For this study, the updated ANZDA (1400–2012 CE) reported by Cook et al. (2018) was used, but excluding the New Zealand grid points.

2.2 Drought and pluvial intensity, area, frequency and duration analyses

To examine the intensity of droughts and pluvials within each NRM cluster, we first conducted a principal component analysis (PCA) on the associated grid cells (Table 1). The high proportion of explained variance captured by the first mode in each NRM provided reassurance of dominant regional signals, which were then plotted to show the year-to-year histories (Fig. 2). We also calculated a drought (and pluvial) area index by determining the proportion of grid cells within each NRM cluster that was experiencing moderate ($1 \leq \text{scPDSI} < 2$), severe ($2 \leq \text{scPDSI} < 3$) or extreme ($\text{scPDSI} \geq 3$) levels of drought or wetting (Fig. S1).

For each NRM cluster, the extreme levels of drought and pluvial intensity and the area affected by extremes were used to compute recurrence intervals over the 1400–2012 CE period, following the methodology of Morales et al. (2020) and as outlined by Mudelsee et al. (2004). Recurrence intervals for the first mode across each NRM cluster were based on the extreme values of the scPDSI (i.e. greater than the 95th percentile or lower than the 5th percentile). A density plot of the time intervals between consecutive extreme dry or consecutive extreme wet events shows that these intervals are not normally distributed in all of the different NRM clusters (Fig. S2 and Table S1), so non-parametric statistical analyses are needed. Kernel density estimation (KDE) is a non-parametric way to estimate the probability density pattern of a random variable. Here, we calculated the Gaussian kernel function using the R-package *'paleofire'* (Blarquez et al. 2014). The *'kdfreq'* routine computed the extreme event frequencies for each NRM region using a Gaussian kernel density estimation procedure based on a defined bandwidth (see Mudelsee 2004 for

Table 1 Analysis of the drought indices (1400–2012 CE) for each NRM cluster (WT Wet Tropics, MN Monsoonal North, EC East Coast, CS Central Slopes, RL Rangelands, MB Murray Basin and SS Southern Slopes)

(a)

Record		Principal components			Total variance explained (%)
		PC1	PC2	PC3	
Cluster	WT	52	13	7	72
	MN	48	19	7	74
	EC	72	5	3	80
	CS	74	7	3	84
	RL	57	8	6	71
	MB	63	8	5	76
	SS	47	21	6	74
	Average	59	12	5	

(b)

Record		Cluster							
		WT	MN	EC	CS	RL	MB	SS	
Cluster	WT	–	0.801	0.519	0.443	0.552	0.385	0.399	Entire time period: 1400–2012 CE
	MN	0.858	–	0.470	0.319	0.709	0.394	0.286	
	EC	0.643	0.633	–	0.891	0.609	0.699	0.823	
	CS	0.613	0.784	0.862	–	0.672	0.809	0.847	
	RL	0.755	0.780	0.703	0.771	–	0.810	0.590	
	MB	0.487	0.430	0.702	0.502	0.784	–	0.852	
	SS	0.380	0.276	0.749	0.752	0.557	0.859	–	
‘Instrumental’ period: 1900–2012 CE									

(a) Principal component analysis showing the amount of variance explained

(b) Cross-correlations between the PC1 indices of each cluster for both the entire reconstructed time period (1400–2012 CE) and only over the instrumental period (1900–2012 CE). This was done to help demonstrate the stability of the cross-correlation relationships

details). Confidence bands at the 95% level were obtained using 1000 bootstrap simulations to interpret these estimates better. The approach is similar to that described by Morales et al. (2020) for the South American Drought Atlas (SADA). Pseudo-replicated values lying outside the observational window are used in the package to correct potential edge bias, equivalent to ‘boundary bias reduction’ described in Mudelsee (2014).

One key consideration in this analysis is the bandwidth (*h*) selection, as this determines the bias and variance properties of the occurrence rate of extreme events through time. Bandwidth selection also has large effects on occurrence rate estimation. The choice of a small bandwidth can allow too many variations and will often fail to identify significant events—often described as under-smoothing. In contrast, over-smoothing removes many significant variations in event occurrence rate (i.e. reduces the estimation variance but enhances the bias). We used the Sheather (1991) method to select bandwidth values for each region over the entire time period. The median length of extreme droughts was longer than that of extreme pluvials. We adopted a slightly lower bandwidth (i.e. *h* = 35) than the

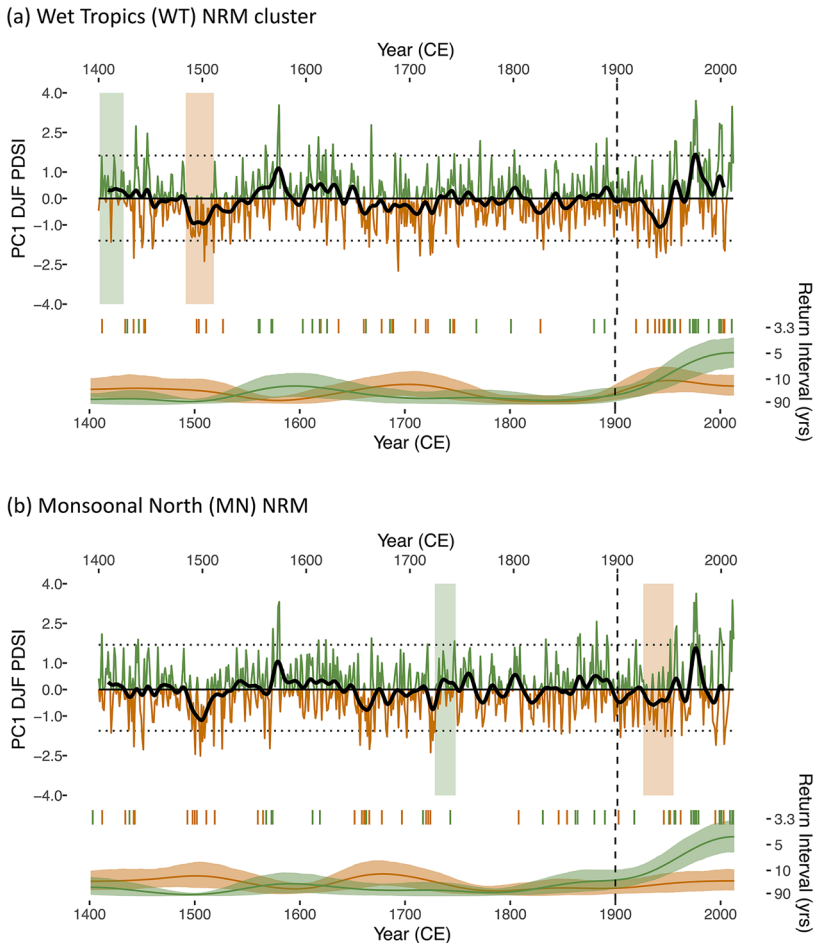
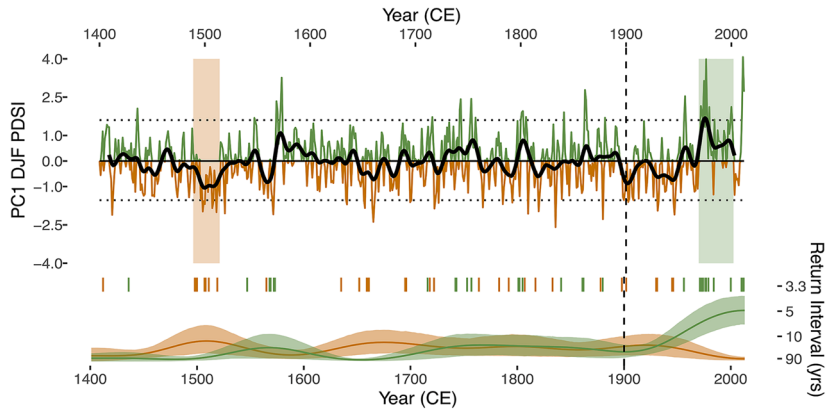


Fig. 2 The drought severity index since 1400 CE for Natural Resource Management (NRM) clusters in eastern Australia. **(a)** Wet Tropics (WT). **(b)** Monsoonal North (MN). **(c)** Rangelands (RL). **(d)** Central Slopes (CS). **(e)** East Coast (EC). **(f)** Murray Basin (MB). **(g)** Southern Slopes (SS). For each cluster, the first principal component (PC1) of the Austral summer (Dec–Feb) drought intensity is plotted (i.e. upper figure) with shading highlighting contiguous periods of time of droughts or pluvials. The 5th and 95th percentile thresholds shown with dotted lines help to denote extreme year occurrences. Those years when extremes were reached are highlighted underneath as a bar chart, and the data are then used to plot the time-varying frequency of extreme occurrences (i.e. return intervals). Dashed vertical line indicates the start of the instrumental period. *Note* The same process was applied to the relative areas of the NRM clusters under drought or pluvial conditions (i.e. $\text{scPDSI} > |2|$) with the figures placed in Supplementary (Fig. S1)

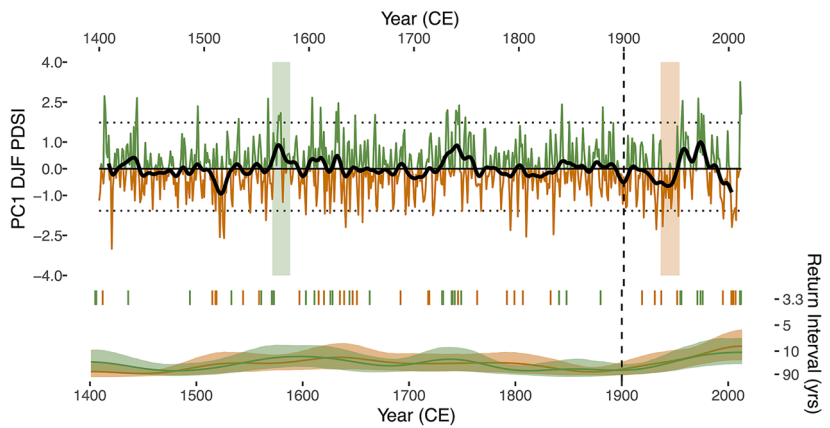
median for the extreme pluvials before running the ‘*kdffreq*’ routine. The rationale for this was to suppress potential extrapolation effects, further reduce the bias and achieve methodological consistency for all the NRM regions. The slightly lower bandwidth approach is also consistent with Mudelsee et al. (2003) advice to under-smooth slightly.

The duration of consecutive dry or wet years was compiled for each NRM cluster (Fig. S3). Definitions of what determine a drought event vary in terms of both input data (e.g. scPDSI versus precipitation in the observed record) and criteria (Cook et al. 2022).

(c) Rangelands (RL) NRM cluster



(d) East Coast (EC) NRM cluster



(e) Central Slopes (CS) NRM cluster

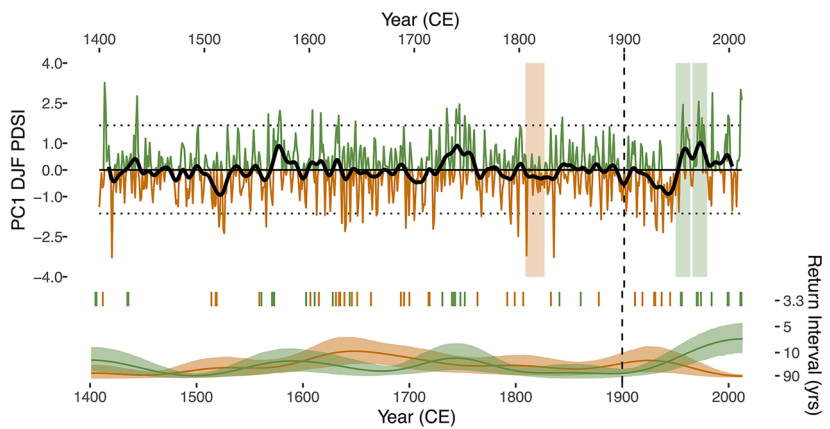
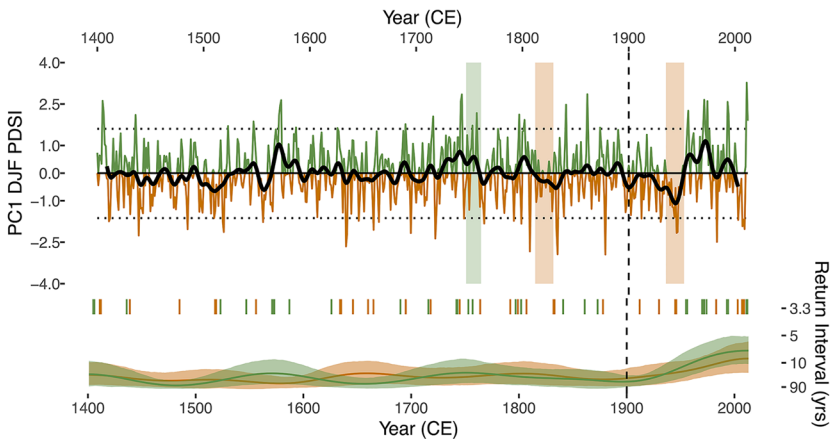


Fig. 2 (continued)

(f) Murray Basin (MB) NRM cluster



(g) Southern Slopes (SS) NRM cluster

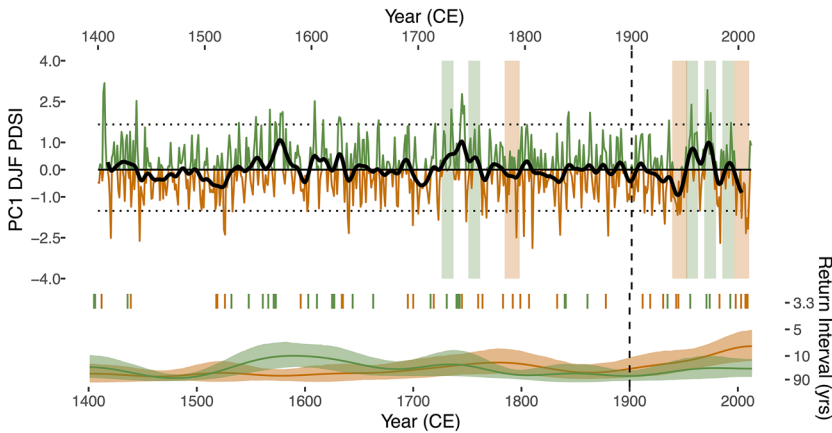


Fig. 2 (continued)

We have adopted a drought definition similar to that described in Coats et al. (2013) for scPDSI data (termed S2E2), with a drought commencing after 2 consecutive years of negative anomalies and continuing until 2 successive years of positive anomalies. The same criteria (but of opposite conditions) were used for determining a pluvial event.

2.3 Emerging hot spot analysis and identification of potential drought refugia

Spatial pattern analysis can assist with the consistent identification of regions historically vulnerable to or naturally buffered from climate extremes. This information can help identify priority areas for management intervention. For example, regions naturally buffered from recurring drought may offer a refugia for endangered species impacted by drought elsewhere. Pattern analysis, therefore, offers important evidence-based opportunities for

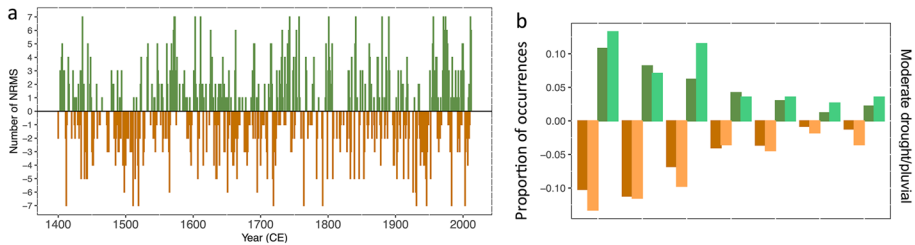


Fig. 3 Summary of the co-occurrence of droughts and pluvials across multiple NRM clusters. **(A)** Year-by-year number of NRM clusters concurrently at more than 1σ above (i.e. pluvial event; green) or below normal (i.e. drought event; brown). **(B)** The proportion of occurrences (i.e. number of times more than 1σ above or below normal over the entire record of 613 years) by the number of NRM clusters. Note darker shading of green and brown reflects the proportions occurring during the palaeo record of 1400–1899 CE, while the lighter shading covers the ‘instrumental’ era of 1900–2012 CE

conservation management. This study identifies spatiotemporal variability in the gridded scPDSI using a space–time pattern mining method known as ‘emerging hot spot analysis’ (ArcGIS; Fig. 3). This method identifies statistically significant ‘hot spots’—in our case frequent drought, and ‘cold spots’—less frequent drought (refugia).

The emerging hot spot method generates trends in point density (counts), and therefore, the scPDSI had first to be converted to a binary (1, 0) data cube (known as a space–time cube). Here, we focus on trends in severe to extreme drought (i.e. scPDSI < -3), so the data cube was prepared by allocating all scPDSI < -3 to a value of 1 and all other scPDSI values to zero. Only data from 1900 to 2012 (i.e. instrumental period) were used to identify hot and cold spots. This approach was taken so that we could identify potential refugia (cold spots) that have been less affected by drought than the surrounding regions during the instrumental period. We then tested the stability of these refugia by selecting four cold spots as examples and assessed their drought history over time by comparison to the entire 612-year record of the ANZDA.

The emerging hot spot method utilises a combination of two statistical measures:

- The Getis–Ord G_i^* statistic (Getis and Ord 1992) to identify the location and degree of spatial clustering; and
- The Mann–Kendall trend test (Kendall and Gibbons 1990; Mann 1945) to evaluate temporal trends across the time series.

The Getis–Ord G_i^* statistic measures the intensity of clustering (i.e. in our analysis, counts of scPDSI < -3 through time) for each grid cell relative to its neighbouring grid cells. Specifically, this statistic identifies significant clusters of high values (hot spots) or low values (cold spots) and measures their intensity. It does this by generating Z-scores and p-values for each cell, indicating whether the scPDSI counts in a given cell are statistically clustered compared to the scPDSI counts in neighbouring cells and across the entire spatial domain. A Z-score above 1.96 signifies a statistically significant ‘hot spot’, and a Z-score below -1.96 represents a statistically significant ‘cold spot’ at a significance level of $p < 0.05$. The larger the Z-score, the more intense the clustering of values. A K-means clustering of eight spatial neighbours (grid cells) and a neighbourhood

timestep of 25 years (period over which counts were accumulated) was adopted for the analysis after initial sensitivity testing of these parameters. The Getis–Ord G_i^* statistic equations are detailed in Getis and Ord (1992).

The Mann–Kendall statistic assesses whether a statistically significant temporal trend exists through each grid cell's 113-year time series of Z-scores resulting from the Getis–Ord G_i^* statistic. The Mann–Kendall statistic analyses the rank correlations between data values and their corresponding time points to determine the long-term data series' trend (as detailed in Mann in 1945). This test employs two key parameters: the significance level of trend denoted as (Z), and the slope of the trend represented as (S) to gauge the significance and direction of changes within the data. The significance level helps determine whether the observed trend holds statistical significance, while the slope conveys the magnitude and direction of this trend.

The cluster and trend results from the Getis–Ord G_i^* and Mann–Kendall statistics are then used to categorise each grid cell. The results are symbolised with one of the six hot and cold spot categories describing the statistical significance of hot or cold spots and the location's trend over time, as detailed below (Fig. 3).

- A sporadic hot spot means that this cell/region has a history of severe droughts scattered throughout the modern (since 1900) record, including the most recent timestep. Notably, there are no 25-year periods (the selected neighbourhood timestep) in the record without a severe drought.
- An oscillating hot spot has a history of severe droughts scattered throughout the modern (since 1900) record, including the most recent timestep. In contrast with the sporadic hot spot, this region has at least one 25-year period without severe drought.
- A sporadic cold spot indicates a region that has not experienced a severe drought in the past 25 years and has a history of being less exposed to severe drought.
- An oscillating cold spot has also not experienced a severe drought in the past 25 years. However, it has experienced periods of extreme drought in the past (more so than the sporadic cold spot).
- A consecutive cold spot indicates a region where the last two timesteps (50 years) have been free from drought; but severe drought has occurred before this at some point.
- No pattern detected indicates no significant trend in drought occurrence for this region/cell.

Potential drought refugia were identified as any region within the three cold spot categories (consecutive, sporadic and oscillating) (Fig. 3). Collectively, this represents a region that has fewer occurrences of severe to extreme drought than other nearby regions. The combined cold spot information was then overlaid with the Australian Landuse and Management Classification V8 (ALUMV8) to identify natural regions that have offered a buffer from drought over the past century. Examples of potential refugia were then identified for further analysis, and the extended (612-year) time series of drought occurrence was extracted at that location. The incidence of drought across the pre-instrumental record provided through our NRM analysis of the ANZDA record was then compared to the modern period.

3 Results

3.1 Drought and pluvial intensity, area, frequency and duration for NRM clusters

The principal component analysis (PCA) of each NRM cluster showed that around 60% of the variability is captured by the first principal component (Table 1a). This provides a level of reassurance that the grid cells within each cluster are not highly heterogeneous in their drought responses. The highest value was from the CS (74%), and the lowest was from the SS (47%). Only three clusters had a second principal component value above 10% (SS, MN and WT), likely reflecting the more diverse local landscapes compared to the other regions.

The correlations between paired NRM clusters broadly showed a latitudinal response, with the northern-most (i.e. WT and MN) and southern-most (i.e. SS) clusters being the least correlated to each other (Table 1b). Adjoining clusters tended to have higher correlations than those more distant. The results in Table 1b also show that there were no noticeable declines in the correlations from the recent period (i.e. 1900–2012 CE) compared to those from the entire period (i.e. 1400–2012 CE). This demonstrates that the relationships are not unique to the recent ‘instrumental’ period and that temporal consistency, or stability, exists over the entire window of time.

Each cluster’s reconstructed drought intensity record is presented in Fig. 2, with the corresponding record for drought areas provided in Supplementary (Fig. S1). A summary of the results from each cluster is as follows (arbitrarily going from north to south):

- Wet Tropics (WT) cluster. The only protracted pluvial event appears at the start of the record, after which there is a period of increased aridity centred around 1500 CE. Pluvial events then returned to dominate late in the 16th century. A noticeable quiescent period appears late in the 18th and entire 19th centuries. There is greater variability in the 20th century and a marked increase in the pluvial recurrence rate.
- Monsoonal North (MN) cluster. Pronounced droughts occurred around 1500 CE, with other less conspicuous droughts ~1650 CE and the early 18th century. Substantial pluvial periods are evident in the late 16th century and the 1970s. Temporally scattered and infrequent extreme events occurred from the mid-18th and 19th centuries before a distinct period of extreme pluvials beginning in the 1920s that are reflected in the reduced recurrence interval for pluvial events.
- Rangelands (RL) cluster. An intense drought episode is centred around 1500 CE, with a dramatic switch from persistent drought conditions to strong pluvial events in the 1580s. Drought events seem to dominate the early 20th century before a mid-century transition to persistent pluvials with a number of extreme wet events. As for MN and WT, the recurrence interval for pluvial conditions has significantly reduced since the middle of the 20th century.
- East Coast (EC) cluster. A pronounced pluvial phase is seen in the late 1500s, during the early-mid 1700s and after 1950. A prolonged and well-documented (e.g. Verdon-Kidd and Kiem 2009) drought occurred during the Second World War. The frequency of extreme events is relatively unremarkable, although both extreme droughts and pluvials appear more common from the mid-20th century. However, neither the recurrence of extreme drought nor pluvial events have statistically changed during the 600 years.
- Central Slopes (CS) cluster. Similar to the Rangelands, severe drought can be observed in the early 1500s, followed by extended pluvial conditions during the latter part of the 16th century. There was a pronounced pluvial period in the early-mid

1700s and again from ~1950s to 70s, preceded by extended drought conditions. The return interval for extreme pluvials has sharply decreased from the mid-20th century but less clearly than for the WT and MN clusters.

- Murray Basin (MB) cluster. Prominent pluvial events are evident in the late 16th century, as is an extended pluvial period during the first half of the 18th century. The Second World War drought stands out in terms of its magnitude and duration, and both extreme pluvials and droughts appear to be more frequent towards the latter part of the 20th century, although their recurrence intervals have not significantly changed compared to the previous centuries.
- Southern Slopes (SS) cluster. Drought was most persistent ~1500, the Second World War and then from the 1990s. Drought in the latter period is most pronounced across the eastern seaboard NRM regions. There are distinct pluvial episodes in the mid-late 16th century, the mid-18th century and through much of the middle of the 20th century. Although recent drought conditions have become more frequent since 1990, their recurrence is not yet statistically distinct from the rest of the 600-year record.

The persistence of pluvial conditions in the more northern NRM clusters (WT, MN, RL and CS) over the second half of the 20th century is notable in the context of the past 600 years. While the MDB and EC also exhibit pluvial conditions in the 1950s and 1970s in particular, these have been less persistent than for the northern and inland NRMs. At the same time, (with the exception of the 2011–12 period), decreasing scP-DSI indicates increasingly dry conditions in the MDB and SS, although notably, these conditions do not appear more extreme than those that have previously been experienced in these NRMs (while still being ranked in the worst 5%). The mid-1700s stand out as a relatively wet period for CS, EC, MDB and SS; and the period ~1500 CE was generally dry across the eastern seaboard (slightly muted for MDB and SS). These patterns are reinforced by the relative areas of each NRM experiencing drought/pluvial conditions at any one time. The 20th century is particularly notable for the relatively large areas within each NRM concurrently experiencing drought/pluvial conditions.

In most cases, the duration of droughts longer than 5 years is not well represented in the instrumental period (Fig. S3). The main exception to this is WT, and to a lesser extent, CS. The duration of pluvial periods across the pre-1900 period is reasonably well represented by their duration, particularly in the MN and MB. The largest differences between the duration expressed in the instrumental compared to the pre-1900 period are for the RL (droughts longer than 10 years) and EC (droughts longer than 4 years; Fig. S3).

A summary of the co-occurrence of droughts and pluvials across multiple NRM clusters is shown in Fig. 3. For each NRM cluster, we first selected only the wet (or dry) years that were more than one standard deviation (i.e. $\geq 1\sigma$) above (below) normal. The number of NRM clusters meeting these criteria for any 1 year was then plotted (Fig. 3a). Although not clearcut, there does appear to be some oscillation between periods with multiple NRMs being either wet or dry (e.g. wet around 1720s CE and dry around 1500 CE). Finally, a comparison was made of the general co-occurrence pattern between the palaeo record (i.e. 1400–1899 CE) and the instrumental period (i.e. 1900–2012 CE) (Fig. 3b). The pattern shows the recent instrumental period to have experienced more large-scale events than the pre-1900 period.

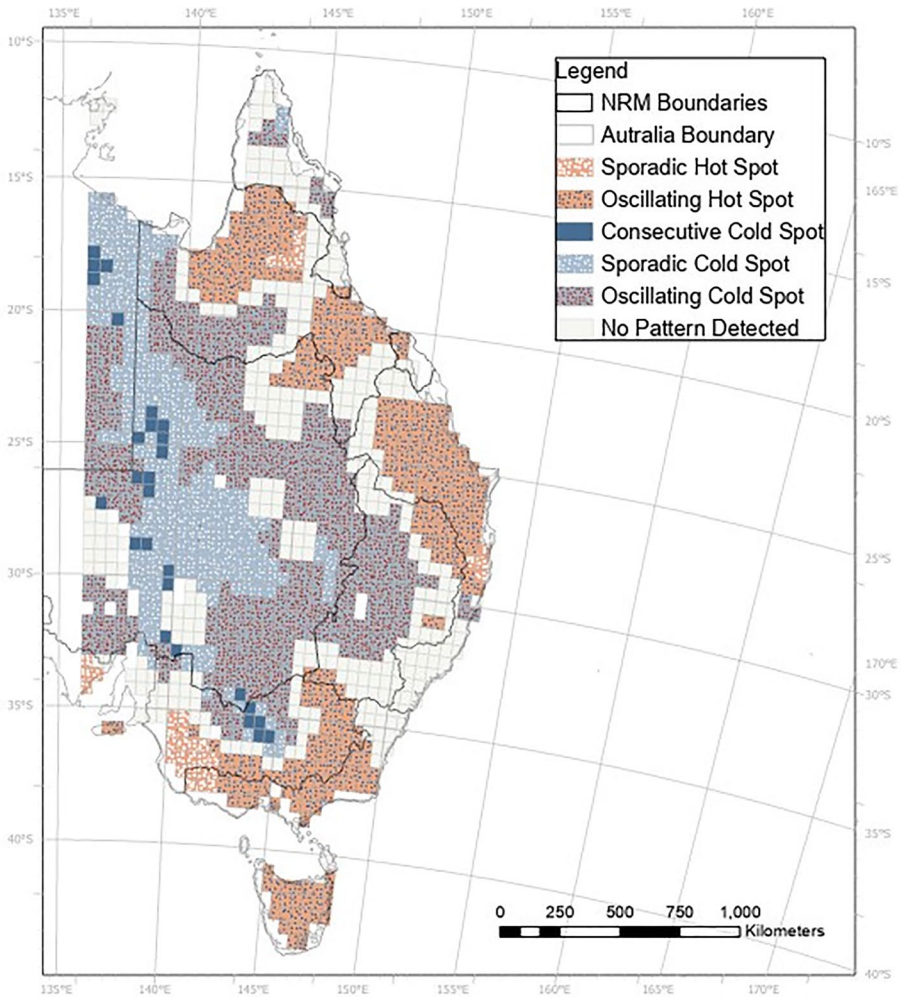


Fig. 4 Emerging hot spot analysis (1900 CE onwards) of the eastern Australian Drought Atlas spatial field indicating areas with more severe droughts than surrounding grid cells (i.e. hot spots) or the reverse situation (i.e. cold spots). The latter are thought to potentially indicate refugia from severe droughts

3.2 Emerging hot spots and the identification of potential drought refugia

The emerging hot spot analysis identified statistically significant hot (i.e. often impacted by drought) and cold (i.e. infrequently impacted by drought) spots for the instrumental period across the NRMs (Fig. 4). Overall, the coastal NRMs feature significant hot spots, predominantly oscillating, during this period (except for the WT), meaning that drought has been a recurrent feature in these regions during the most recent century. In contrast, the interior NRMs are mostly classified as cold spots (absence of drought in the last timestep and overall few severe droughts prior to that). A notable exception for the EC NRM is the region around Port Macquarie to Coffs Harbour, which is classified as a cold spot (i.e. fewer severe droughts; see Fig. 5, cold spot C). One reason that the interior NRMs tend to have fewer droughts is that this region experiences overall lower variability in the scPDSI

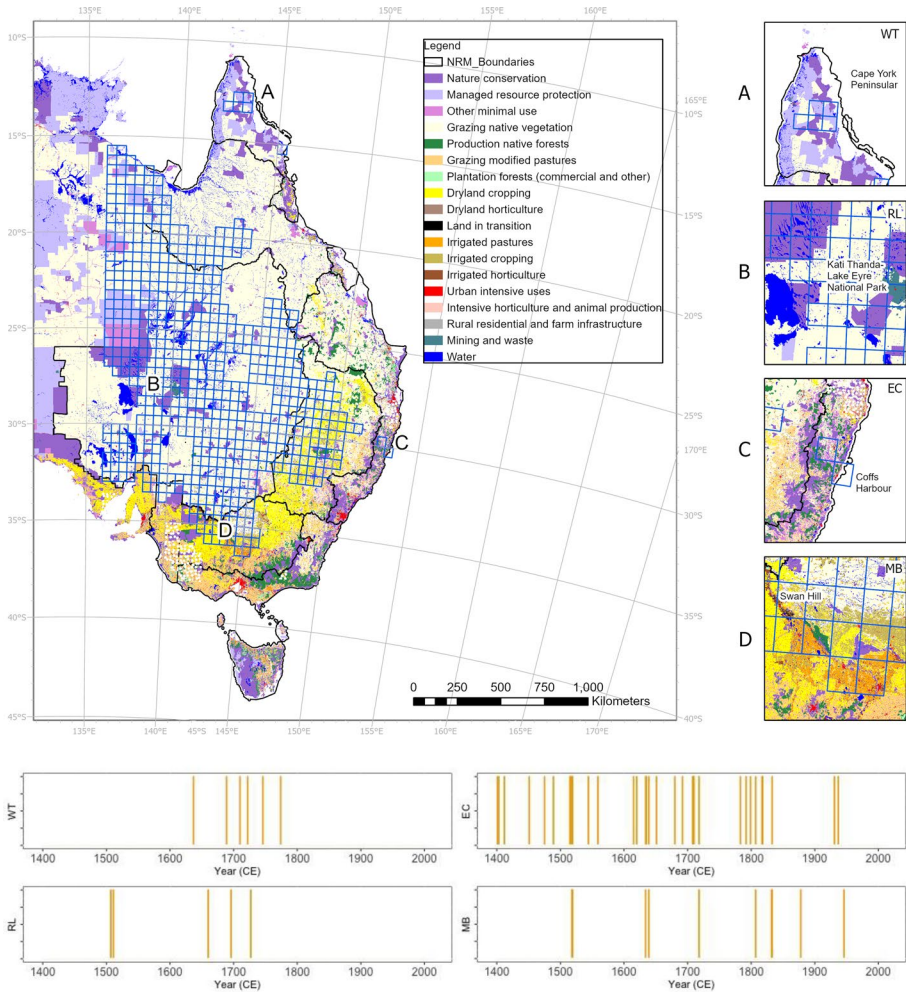


Fig. 5 Map showing the different land-use classifications overlaid with ‘cold spots’ (blue grid cells; redrawn from Fig. 4). Detailed enlargements of four chosen ‘cold spot’ examples (A, B, C, D) found in four different NRM clusters with varying land-use classifications, are shown on the right side of the figure. For each example, the occurrence of significant drought events throughout the entire reconstructed record is then shown in the four lower panels

values (Fig. S4). That is, while this region is more arid, the climate departs from this normal state less often, and as such the scPDSI is more frequently in the ‘normal’ range.

A large proportion of cold spots are located within the cropping and grazing lands of the interior NRMs, particularly the RL (Fig. 5). From an agricultural perspective, this is useful to explore further; however, here, we focus on potential drought refugia located within, or close to, nature conservation, managed resource protection or minimal use (denoted by mauve/purple colour land use). This is because such regions are particularly important to the ecological communities they support. Four example refugia were chosen for further analysis, one from the WT in far North Queensland (Panel A), one from the RL

around Lake Eyre National Park (Panel B), another from the Coffs Harbour region of the EC (Panel C) and a final site in the MB near Swan Hill (Panel D, which is mixed land use but does include Murray Valley National Park). The time series of severe drought events over the entire ANZDA ~600-year period were extracted for these regions (lower panels of Fig. 5). The results show that, for the WT and RL cold spot examples (Fig. 5), similar to the instrumental period, the earlier occurrence of severe droughts was relatively rare, but both regions did still experience severe drought during the 1700s. Otherwise, these two locations may represent relatively stable drought refugia (based on the ANZDA data). Similarly, although severe drought has occurred more regularly for the MB location, the frequency is similar to the instrumental period (~1 per 100 years), meaning that the ecosystems have likely evolved under a matching envelope of drought variability over the 600 years. However, this is not the case for the EC site near Coffs Harbour, which highlights that drought has likely occurred much more frequently before 1850 than it has since. Indeed, the occurrence of severe drought prior to 1850 is substantially higher than in the instrumental period.

4 Discussion

Global climate change poses a significant threat to ecological communities already modified by the human footprint. In the Australian context, this is taking place against the backdrop of an extremely variable climate. Recent trends in extremes have indicated that much of the southeast of Australia has experienced a shift towards drier conditions (Murphy and Timbal 2008), but it is impossible to assess how unusual this is without delving further into the past. Here, we present a 600-year assessment of wetting and drying trends across eastern Australia to assist in placing these trends in context. Our analysis confirms that the Southern Slopes has experienced increasingly dry conditions and a decrease in pluvials over the second half of the 20th century; however, this was found to be within the bounds of past variability and similar to the early 1500s. In contrast, the persistence of pluvial conditions in the Wet Tropics over the second half of the 20th century, a feature consistent with all of the more northern NRMs, was found to be unique within this long-term context. These patterns are also reinforced by the relative area results (Fig. S1). Each NRM contains a unique pluvial and drought history record punctuated by a severe pluvial period during the mid-1700s across all the NRM clusters, and the period around 1500 was marked by widespread severe drought.

The relative lack of available tree-ring chronologies on the Australian mainland that could be used to produce the ANZDA is an important caveat for our analyses and the resulting trends we have identified. A large proportion of the chronologies come from New Zealand and Tasmania, with an additional subset in northern Australia. As such, it is helpful to compare our reconstructed drought index for each NRM cluster (i.e. PC1) with other annual-resolution hydroclimate reconstructions in eastern Australia (Table 2). Most of these are for slightly different seasons to the ANZDA and are derived from a range of proxies, including both remote and in situ (described in Table 2). Four of the twelve reconstructions, identified in Table 2a, shared some tree-ring proxies with the current study and, therefore, cannot be considered strictly independent, and as perhaps to be expected, they were all significantly correlated to our reconstructions (Table 2b; Allen et al. 2015; Freund et al. 2017; Gallant and Gergis 2011; Higgins et al. 2022). Both the Wet Tropics and Monsoonal North clusters were significantly correlated to all but one of the five independent

Table 2 Comparisons of the reconstructed drought index for each NRM cluster (i.e. PCI) to other annual-resolution publications focused on hydroclimate reconstructions in eastern Australia

Record	Hydroclimate variable reconstructed	Seasonality	Proxy type	Common overlap (years)	Shared tree-ring proxies
1	WT MN EC CS RL MB SS	Oct–Mar Oct–Mar Oct–Mar Oct–Mar Oct–Mar Oct–Mar Oct–Mar	Multi-proxy Multi-proxy Multi-proxy Multi-proxy Multi-proxy Multi-proxy Multi-proxy	1400–1999 1737–1999 1400–2009 1400–2009 1607–1999 1400–1999 1635–1999	Yes Yes Yes Yes Yes Yes Yes
2	Burdekin River Pioneer River Fitzroy River Herbert River Queensland	Oct–Sep Oct–Sep Oct–Sep Oct–Sep Oct–Mar	Corals Corals Corals Corals Corals	1648–2011 1660–1983 1678–1983 1785–1983 1685–1981	No No No No No
3	Alligator River	Sep–Aug	Multi-proxy	1470–1977	No
4	Daly River	Sep–Aug	Tree-rings	1413–2005	Yes
5	Yungaburra NP	Mar–Jun	Tree-rings	1860–2000	No
6	Lamington NP	Mar–Jun	Tree-rings	1854–2000	No
7	Williams River	Oct–Sep	Ice core	1400–2012	No
8	Southeast Queensland	Jan–Dec	Ice core	1400–2012	No
9	Murray River	Aug–Jul	Multi-proxy	1783–1988	Yes
10	Gallant and Gergis (2011)	Jul–Jun	Multi-proxy	1684–1980	No
11	Ho et al. (2015)	Dec–Feb	Tree-rings	1400–2007	Yes
12	Lake Burbury				

Table 2 (continued)

Record	Cluster											
		WT	MN	EC	CS	RL	MB	SS				
1	Freund et al. (2017)	WT	0.353									
		MN		0.409								
		EC			0.528							
		CS				0.511						
		RL					0.413					
		MB						0.251				
		SS									0.274	
2	Lough et al. (2007)	Burdekin River	0.384	0.377								
		Pioneer River	0.319	0.333								
		Fitzroy River	0.063	0.085								
		Herbert River	0.308	0.290								
		Queensland	0.274	0.281								
		Alligator River	0.254	0.140								
		Daly River										
		Yungaburra NP	0.190									
		Lamington NP			0.240							
		Williams River			0.081							
		Southeast Queensland			0.009							
		Murray River						0.407				
		Murray River						0.091				
		Lake Burbury										-0.240*

(a) Summary details of earlier publications

(b) Correlations between our reconstructions to the previous publications for the common associated areas. *Note* Pearson correlation significance: $p > 0.01$ (bold); $p > 0.05$ (normal font) and $p < 0.05$ (not significant, italics);

*The PC2 correlation was 0.312 ($p > 0.01$)

coral-based reconstructions by Lough (2007, 2011). Our East Coast cluster reconstruction was significantly correlated with the independent local tree-ring-based reconstruction by Heinrich et al. (2009). However, our East Coast reconstruction was not correlated with those of the Williams River Catchment (Tozer et al. 2016) or the Southeast Queensland rainfall station (Australian Bureau of Meteorology, gauge number 40082; Kiem et al. 2020) (Table 2b). Both of these reconstructions are based on summer sea-salt concentration in the Antarctic Law Dome ice-core (LDss) and as recently pointed out by Jong et al. (2022), the LDss record has both missing values and cumulative age uncertainties. These factors could have affected their correlations to our tree-ring-based reconstructions. It is notable that the two ice-core-based reconstructions were extremely highly correlated with one another (Pearson correlation of 0.98) and neither was correlated with the Heinrich et al. (2009) reconstruction (Pearson correlations of -0.116 and -0.095 , respectively).

The Murray Basin cluster did not correlate with the rainfall reconstruction by Ho et al. (2015). However, about half of the common overlapping time period of their reconstruction with ours was based solely on a low-frequency aridity index (wet/dry) combined with stochastically derived annual rainfall data, which would explain the poor correlation at the annual timescale. We believe the negative correlation between the PC1 of the Southern Slopes (SS) cluster, and the Allen et al. (2015) lake in Tasmania is a result of the island's contrasting East–West climate. However, SS PC2 was strongly positively correlated and is more related to the eastern part of Tasmania, which is more climatically similar to the northern part of SS (compared to western Tasmania).

In summary, the scPDSI NRM series correlates significantly with a range of other rainfall and streamflow reconstructions for eastern Australia and those that do not have been identified as either incompatible (e.g. Ho et al. 2015) or potential dating issues (e.g. Tozer et al. 2016 and Kiem et al. 2020). This gives us some confidence in the wetting and drying signatures we have identified, as well as the drought refugia analysis.

Drought refugia have high ecological significance due to their role as natural buffers against drought (Selwood and Zimmer 2020). Our analysis identifies the New South Wales North Coast (northern EC NRM) as a potential drought refugium based on the post-1900 CE period. This is one of Australia's most ecologically diverse regions, hosting World Heritage listed Gondwanan rainforests, major river catchments and numerous wetlands and beaches. In addition to a changing climate, the North Coast faces significant anthropogenic pressures from rapid land-use change. Greater Coffs Harbour is at the centre of this urban growth, with a projected $\sim 35\%$ increase in population by 2041. Such growth will result in an expansion of intensive land use and increased competition for resources (e.g. water for industry and residential), all at a cost to the natural landscape. While this applies to most NSW coastal cities, the Coffs Harbour region is of particular concern due to its refugium status. However, the pre-instrumental period drought data for this region show the regular occurrence of severe drought. This raises an important issue. Will treating the region as a drought refugium based only on ~ 100 years of data when the palaeo-evidence suggests that the region is not an actual drought refugium lead to suboptimal ecological outcomes? We acknowledge that ground truthing with local palaeoclimate data is required to determine this with more certainty; however, at the time of writing, such data do not exist. The analysis presented here is an important reason to initiate this process.

Although we have illustrated the use of the tree-ring-derived drought atlas to some specific areas for conservation, other applications are equally possible. One specific use is to inform climate risk and variability estimation (informing on 'black swan events') for insurance indexes. Bell et al. (2013) have demonstrated the utility of longer-term climate histories from the Monsoon Asia Drought Atlas (MADA) and the North American Drought

Atlas (NADA) for index insurance applications. The improved characterisation of the distribution of climate events from longer time series helped refine risk estimates for the insurance provider and contract holder. Recently, Waha et al. (2022) highlighted seasonal rainfall trends for Australian agriculture, with future projections for the wheat belt showing a strong decline in western Australia and a more mixed result for the eastern sector. The study calls for a future re-evaluation of the trend analyses for eastern Australia as data become available—something a tree-ring-based drought atlas could contribute towards. In another example, Tellman et al. (2022) suggested that improvements to flood risk estimates based on satellite time series of inundation are possible, with examples from Bangladesh and Rio Salado (Argentina). Spatial fingerprints of extreme pluvials could be used from a drought atlas in a similar manner, with the key advantage being a better-constrained return period estimation.

There is a clear need to develop other high-quality tree-ring datasets for mainland Australia, although this has so far been hampered by a lack of species deemed suitable for dendrochronology (Haines et al. 2016). Research into additional species is currently underway and will be vital for further verifying the identification of hot and cold spots. Nevertheless, the type of information we have been able to produce here with what is already available in the ANZDA is valuable, and our analyses indicate the type of regionally relevant information that can already be extracted.

5 Conclusions

The application of tree-ring networks for spatial field drought reconstruction (i.e. a drought atlas) provides a wealth of information that can be extracted at scales relevant to land managers. Part of their usefulness lies in the fact that they extend over much longer timescales than available instrumental records and are, therefore, better able to constrain error estimates of extreme event recurrence. Their annual resolution means that the information that can be extracted is available at a resolution most useful for resource planning. In this paper, we have explored the drought and pluvial frequency trends for East Australian Natural Resource Management (NRM) clusters based on the 600-year ANZDA. The results showed some sustained multi-decadal periods of wetting or drying in common across the different NRM clusters. Some wet–dry geographic ‘seesaw’ periods also appeared between eastern to central and southern NRMs. In most cases, the durations of droughts and pluvials that have occurred since 1400 CE are not well represented within the instrumental data period. This helps demonstrate that 20th century instrumental records alone are limited in their capabilities for assessing and preparing/managing for changes in the recurrence of extreme hydroclimatic conditions.

Importantly, emerging hot spot analysis has revealed that some areas appearing to be naturally buffered from drought during the instrumental period might not be when the longer 600-year record is considered. Our data show that basing assessment of what constitutes a flora/fauna refugia on only the past century is inadvisable and may simply increase vulnerability to change. Long-term data are essential for determining what may and may not be refugia. Although our results demonstrate some of the value of long-term proxy climate data available from a drought atlas, we know that the network of tree-ring predictors mostly came from outside the NRM clusters. The independent verification with some other

studies does support our general findings but also highlights the importance of investing in future efforts to obtain more local records.

Supplementary Information The online version contains supplementary material available at <https://doi.org/10.1007/s11069-023-06288-0>.

Acknowledgements We would like to thank the Anthony Kiem and Carly Tozer for providing their reconstructions referred to in this paper.

Funding This work was supported by the Australian Research Council (ARC) Centre of Excellence in Australian Biodiversity and Heritage (Grant No. CE170100015). Kathy Allen is supported by an ARC Future Fellowship (Grant No. FT200100102).

Declarations

Conflict of interest The authors have not disclosed any competing interests.

Open Access This article is licensed under a Creative Commons Attribution 4.0 International License, which permits use, sharing, adaptation, distribution and reproduction in any medium or format, as long as you give appropriate credit to the original author(s) and the source, provide a link to the Creative Commons licence, and indicate if changes were made. The images or other third party material in this article are included in the article's Creative Commons licence, unless indicated otherwise in a credit line to the material. If material is not included in the article's Creative Commons licence and your intended use is not permitted by statutory regulation or exceeds the permitted use, you will need to obtain permission directly from the copyright holder. To view a copy of this licence, visit <http://creativecommons.org/licenses/by/4.0/>.

References

- Allen KJ, Nichols SC, Evans R, Cook ER, Allie S, Carson G, Ling F, Baker PJ (2015) Preliminary December–January inflow and streamflow reconstructions from tree rings for western Tasmania, southeastern Australia. *Water Resour Res* 51(7):5487–5503. <https://doi.org/10.1002/2015wr017062>
- Bell AR, Osgood DE, Cook BI, Anchukaitis KJ, McCarney GR, Greene AM, Buckley BM, Cook ER (2013) Paleoclimate histories improve access and sustainability in index insurance programs. *Glob Environ Chang* 23(4):774–781. <https://doi.org/10.1016/j.gloenvcha.2013.03.003>
- Blarquez O, Vanni re B, Marlon JR, Daniau A-L, Power MJ, Brewer S, Bartlein PJ (2014) paleofire: an R package to analyse sedimentary charcoal records from the Global Charcoal Database to reconstruct past biomass burning. *Comput Geosci* 72:255–261. <https://doi.org/10.1016/j.cageo.2014.07.020>
- Burnette DJ (2021) The tree-ring drought atlas portal: Gridded drought reconstructions for the past 500–2,000 years. *Bull Am Meteor Soc* 102(10):953–956. <https://doi.org/10.1175/BAMS-D-20-0142.1>
- CSIRO, Bureau of Meteorology (2015) Climate change in Australia information for Australia's natural resource management regions: technical report, CSIRO and Bureau of Meteorology, Australia p 216
- Coats S, Smerdon JE, Seager R, Cook BI, Gonz lez-Rouco JF (2013) Megadroughts in southwestern North America in ECHO-G millennial simulations and their comparison to proxy drought reconstructions. *J Clim* 26(19):7635–7649. <https://doi.org/10.1175/JCLI-D-12-00603.1>
- Cook BI, Palmer JG, Cook ER, Turney CSM, Allen K, Fenwick P, O'Donnell A, Lough JM, Grierson PF, Ho M, Baker PJ (2016) The paleoclimate context and future trajectory of extreme summer hydroclimate in eastern Australia. *J Geophys Res Atmos* 121(21):12820–12838. <https://doi.org/10.1002/2016JD024892>
- Cook BI, Smerdon JE, Cook ER, Williams AP, Anchukaitis KJ, Mankin JS, Allen K, Andreu-Hayles L, Ault TR, Belmecheri S, Coats S, Coulthard B, Fosu B, Grierson P, Griffin D, Herrera DA, Ionita M, Lehner F, Leland C, Marvel K, Morales MS, Mishra V, Ngoma J, Nguyen HTT, O'Donnell A, Palmer J, Rao MP, Rodriguez-Caton M, Seager R, Stahle DW, Stevenson S, Thapa UK, Varuolo-Clarke AM, Wise EK (2022) Megadroughts in the common era and the Anthropocene. *Nat Rev Earth Environ* 3(11):741–757. <https://doi.org/10.1038/s43017-022-00329-1>
- Cook BI, Williams AP, Smerdon JE, Palmer JG, Cook ER, Stahle DW, Coats S (2018) Cold tropical Pacific sea surface temperatures during the late sixteenth-century North American megadrought. *J Geophys Res: Atmos* 123(20):11307–11320. <https://doi.org/10.1029/2018JD029323>

- Cook ER, Anchukaitis KJ, Buckley BM, D'Arrigo RD, Jacoby GC, Wright WE (2010) Asian monsoon failure and megadrought during the last millennium. *Science* 328(5977):486–489. <https://doi.org/10.1126/science.1185188>
- Cook ER, Meko DM, Stahle DW, Cleaveland MK (1999) Drought reconstructions for the continental United States. *J Clim* 12(4):1145–1162. [https://doi.org/10.1175/1520-0442\(1999\)012](https://doi.org/10.1175/1520-0442(1999)012)
- Cook ER, Seager R, Kushnir Y, Briffa KR, Buntgen U, Frank D, Krusic PJ, Tegel W, van der Schrier G, Andreu-Hayles L, Baillie M, Baittinger C, Bleicher N, Bonde N, Brown D, Carrer M, Cooper R, Cufar K, Dittmar C, Esper J, Griggs C, Gunnarson B, Gunther B, Gutierrez E, Haneca K, Helama S, Herzig F, Heussner KU, Hofmann J, Janda P, Kontic R, Kose N, Kyncl T, Levacic T, Linderholm H, Manning S, Melvin TM, Miles D, Neuwirth B, Nicolussi K, Nola P, Panayotov M, Popa I, Rothe A, Seftigen K, Seim A, Svarva H, Svoboda M, Thun T, Timonen M, Touchan R, Trotsiuk V, Trouet V, Walder F, Wazny T, Wilson R, Zang C (2015) Old World megadroughts and pluvials during the common era. *Sci Adv* 1(10):e1500561. <https://doi.org/10.1126/sciadv.1500561>
- Cook ER, Solomina O, Matskovsky V, Cook BI, Agafonov L, Berdnikova A, Dolgova E, Karpukhin A, Krysh N, Kulakova M, Kuznetsova V, Kyncl T, Kyncl J, Maximova O, Panyushkina I, Seim A, Tishin D, Wazny T, Yermokhin M (2020) The European Russia drought atlas (1400–2016 CE). *Clim Dyn* 54(3–4):2317–2335. <https://doi.org/10.1007/s00382-019-05115-2>
- Freund M, Henley BJ, Karoly DJ, Allen KJ, Baker PJ (2017) Multi-century cool- and warm-season rainfall reconstructions for Australia's major climatic regions. *Clim past* 13(12):1751–1770. <https://doi.org/10.5194/cp-13-1751-2017>
- Gallant AJE, Gergis J (2011) An experimental streamflow reconstruction for the River Murray, Australia, 1783–1988. *Water Resour Res* 47(12):W00G04. <https://doi.org/10.1029/2010WR009832>
- Getis A, Ord JK (1992) The analysis of spatial association by use of distance statistics. *Geogr Anal* 24:189–206. <https://doi.org/10.1111/j.1538-4632.1992.tb00261.x>
- Grose MR, Narsey S, Delage FP, Dowdy AJ, Bador M, Boschat G, Chung C, Kajtar JB, Rauniyar S, Freund MB, Lyu K, Rashid H, Zhang X, Wales S, Trenham C, Holbrook NJ, Cowan T, Alexander L, Arblaster JM, Power S (2020) Insights from CMIP6 for Australia's future climate. *Earth's Future* 8(5):e2019EF001469. <https://doi.org/10.1029/2019EF001469>
- Haines HA, Olley JM, Kemp J, English NB (2016) Progress in Australian dendroclimatology: identifying growth limiting factors in four climate zones. *Sci Total Environ* 572:412–421. <https://doi.org/10.1016/j.scitotenv.2016.08.096>
- Heinrich I, Weidner K, Helle G, Heinz H, Vos J, Banks CG (2008) Hydroclimatic variation in Far North Queensland since 1860 inferred from tree rings. *Palaeogeogr Palaeoclimatol Palaeoecol* 270(1–2):116–127. <https://doi.org/10.1016/j.palaeo.2008.09.002>
- Heinrich I, Weidner K, Helle G, Vos H, Lindesay J, Banks JCG (2009) Interdecadal modulation of the relationship between ENSO, IPO and precipitation: insights from tree rings in Australia. *Clim Dyn* 33(1):63–73. <https://doi.org/10.1007/s00382-009-0544-5>
- Higgins PA, Palmer JG, Rao MP, Andersen MS, Turney CSM, Johnson F (2022) Unprecedented high northern Australian streamflow linked to an intensification of the Indo-Australian Monsoon. *Water Resour Res* 58(3):e2021WR030881. <https://doi.org/10.1029/2021WR030881>
- Ho M, Kiem AS, Verdon-Kidd DC (2015) A paleoclimate rainfall reconstruction in the Murray-Darling Basin (MDB), Australia: 1. Evaluation of different paleoclimate archives, rainfall networks, and reconstruction techniques. *Water Resour Res* 51(10):8362–8379. <https://doi.org/10.1002/2015WR017058>
- IPCC (2021) Summary for policymakers. In: *Climate Change 2021: the physical science basis. Contribution of Working Group I to the Sixth Assessment Report of the Intergovernmental Panel on Climate Change*. Masson-Delmotte V, Zhai P, Pirani A, Connors SL, Péan C, Berger S, Caud N, Chen Y, Goldfarb L, Gomis MI, Huang M, Leitzell K, Lonnoy E, Matthews JBR, Maycock TK, Waterfield T, Yelekçi O, Yu R, Zhou B (eds.). Cambridge University Press, Cambridge, United Kingdom and New York, NY, USA, pp 3–32. <https://doi.org/10.1017/9781009157896.001>
- Jong LM, Plummer CT, Roberts JL, Moy AD, Curran MAJ, Vance TR, Pedro JB, Long CA, Nation M, Mayewski PA, van Ommen TD (2022) 2000 years of annual ice core data from Law Dome. *East Antarct Earth Syst Sci Data* 14(7):3313–3328. <https://doi.org/10.5194/essd-14-3313-2022>
- Kiem AS, Vance TR, Tozer CR, Roberts JL, Dalla Pozza R, Vitkovsky J, Smolders K, Curran MAJ (2020) Learning from the past – Using palaeoclimate data to better understand and manage drought in South East Queensland (SEQ) Australia. *J Hydrol: Reg Stud* 29:100686. <https://doi.org/10.1016/j.ejrh.2020.100686>
- Kendall M, Gibbons J (1990) *Correlation methods*, pp 35–38, A Charles Griffin Title. London: Griffin
- Lough JM (2007) Rainfall variations in Queensland, Australia: 1891–1986. *Int J Climatol* 11(7):745–768. <https://doi.org/10.1002/joc.3370110704>

- Lough JM (2011) Great Barrier Reef coral luminescence reveals rainfall variability over northeastern Australia since the 17th century. *Paleoceanography* 26(2):PP2201. <https://doi.org/10.1029/2010PA002050>
- Mann HB (1945) Nonparametric test against trend. *Econometrica* 13:245–259. <https://doi.org/10.2307/1907187>
- Morales MS, Cook ER, Barichivich J, Christie DA, Villalba R, LeQuesne C, Srur AM, Ferrero ME, Gonzalez-Reyes A, Couvreur F, Matskovsky V, Aravena JC, Lara A, Mundo IA, Rojas F, Prieto MR, Smerdon JE, Bianchi LO, Masiokas MH, Urrutia-Jalabert R, Rodriguez-Caton M, Munoz AA, Rojas-Badilla M, Alvarez C, Lopez L, Luckman BH, Lister D, Harris I, Jones PD, Williams AP, Velazquez G, Aliste D, Aguilera-Betti I, Marcotti E, Flores F, Munoz T, Cuq E, Boninsegna JA (2020) Six hundred years of South American tree rings reveal an increase in severe hydroclimatic events since mid-20th century. *Proc Natl Acad Sci U S A* 117(29):16816–16823. <https://doi.org/10.1073/pnas.2002411117>
- Mudelsee M (2014) Extreme value time series. In: *Climate Time Series Analysis. Atmospheric and Oceanographic Sciences Library*, vol 51, pp 217–267. Springer, Cham. https://doi.org/10.1007/978-3-319-04450-7_6
- Mudelsee M, Borngen M, Tetzlaff G, Grunewald U (2003) No upward trends in the occurrence of extreme floods in central Europe. *Nature* 425(6954):166–169. <https://doi.org/10.1038/nature01928>
- Mudelsee M, Börngen M, Tetzlaff G, Grünewald U (2004) Extreme floods in central Europe over the past 500 years: role of cyclone pathway “Zugstrasse Vb.” *J Geophys Res: Atmos* 109:D23101. <https://doi.org/10.1029/2004JD005034>
- Mukherjee S, Mishra A, Trenberth KE (2018) Climate change and drought: a perspective on drought indices. *Curr Clim Change Rep* 4(2):145–163. <https://doi.org/10.1007/s40641-018-0098-x>
- Murphy BF, Timbal B (2008) A review of recent climate variability and climate change in southeastern Australia. *Int J Climatol* 28(7):859–879. <https://doi.org/10.1002/joc.1627>
- Palmer JG, Cook ER, Turney CSM, Allen K, Fenwick P, Cook BI, O’Donnell A, Lough J, Grierson P, Baker P (2015) Drought variability in the eastern Australia and New Zealand summer drought atlas (ANZDA, CE 1500–2012) modulated by the Interdecadal Pacific Oscillation. *Environ Res Lett* 10(12):4002. <https://doi.org/10.1088/1748-9326/10/12/124002>
- Palmer WC (1965) Meteorological drought. US Department of Commerce, Weather Bureau
- Peel MC, McMahon TA, Finlayson BL (2004) Continental differences in the variability of annual runoff—update and reassessment. *J Hydrol* 295(1–4):185–197. <https://doi.org/10.1016/j.jhydrol.2004.03.004>
- Selwood KE, Zimmer HC (2020) Refuges for biodiversity conservation: a review of the evidence. *Biol Cons* 245:108502. <https://doi.org/10.1016/j.biocon.2020.108502>
- Sheather SJ, Jones MC (1991) A reliable data-based bandwidth selection method for kernel density estimation. *J R Stat Soc Series B (methodol)* 53(3):683–690
- Stahle DW, Cook ER, Burnette DJ, Villanueva J, Cerano J, Burns JN, Griffin D, Cook BI, Acuña R, Torbenson MCA, Szejner P, Howard IM (2016) The Mexican drought atlas: tree-ring reconstructions of the soil moisture balance during the late pre-Hispanic, colonial, and modern eras. *Quatern Sci Rev* 149:34–60. <https://doi.org/10.1016/j.quascirev.2016.06.018>
- Taleb NN (2007) *The black swan: the impact of the highly improbable*. Penguin Books, 366pp.
- Tellman B, Lall U, Islam AKMS, Bhuyan MA (2022) Regional index insurance using satellite-based fractional flooded area. *Earth’s Fut* 10(3):e2021EF002418. <https://doi.org/10.1029/2021EF002418>
- Tozer CR, Vance TR, Roberts JL, Kiem AS, Curran MAJ, Moy AD (2016) An ice core derived 1013-year catchment-scale annual rainfall reconstruction in subtropical eastern Australia. *Hydrol Earth Syst Sci* 20(5):1703–1717. <https://doi.org/10.5194/hess-20-1703-2016>
- Tozer CR, Kiem AS, Vance TR, Roberts JL, Curran MAJ, Moy AD (2018) Reconstructing pre-instrumental streamflow in Eastern Australia using a water balance approach. *J Hydrol* 558:632–646. <https://doi.org/10.1016/j.jhydrol.2018.01.064>
- van der Schrier G, Barichivich J, Briffa KR, Jones PD (2013) A scPDSI-based global data set of dry and wet spells for 1901–2009. *J Geophys Res: Atmos* 118(10):4025–4048. <https://doi.org/10.1002/jgrd.50355>
- Verdon-Kidd DC, Kiem AS (2009) Nature and causes of protracted droughts in southeast Australia: comparison between the Federation, WWII, and Big Dry droughts. *Geophys Res Lett* 36(22):L22707. <https://doi.org/10.1029/2009GL041067>
- Verdon-Kidd DC, Hancock GR, Lowry JB (2017) A 507-year rainfall and runoff reconstruction for the Monsoonal North West Australia derived from remote paleoclimate archives. *Glob Planet Change* 158:21–35. <https://doi.org/10.1016/j.gloplacha.2017.09.003>
- Vogel E, Donat MG, Alexander LV, Meinshausen M, Ray DK, Karoly D, Meinshausen N, Frieler K (2019) The effects of climate extremes on global agricultural yields. *Environ Res Lett* 14(5):4010. <https://doi.org/10.1088/1748-9326/ab154b>

- Waha K, Clarke J, Dayal K, Freund M, Heady C, Parisi I, Vogel E (2022) Past and future rainfall changes in the Australian midlatitudes and implications for agriculture. *Clim Change* 170(3–4):29. <https://doi.org/10.1007/s10584-021-03301-y>
- Wittwer G, Waschik R (2021) Estimating the economic impacts of the 2017–2019 drought and 2019–2020 bushfires on regional NSW and the rest of Australia. *Aust J Agric Resour Econ* 65(4):918–936. <https://doi.org/10.1111/1467-8489.12441>

Publisher's Note Springer Nature remains neutral with regard to jurisdictional claims in published maps and institutional affiliations.

Authors and Affiliations

Jonathan G. Palmer^{1,2}  · **Danielle Verdon-Kidd**³ · **Kathryn J. Allen**^{1,4} · **Philippa Higgins**¹ · **Benjamin I. Cook**^{5,6} · **Edward R. Cook**⁵ · **Christian S. M. Turney**^{1,2,7} · **Patrick J. Baker**⁸

✉ Jonathan G. Palmer
j.palmer@unsw.edu.au

¹ Australian Research Council (ARC) Centre of Excellence in Australian Biodiversity and Heritage (CABAH), School of Biological, Earth and Environmental Sciences (BEES), University of New South Wales (UNSW), Sydney, NSW 2052, Australia

² Chronos 14Carbon-Cycle Facility, Mark Wainwright Analytical Centre (MWAC), University of New South Wales (UNSW), Sydney, NSW 2052, Australia

³ School of Environmental and Life Sciences, University of Newcastle, Callaghan, NSW 2308, Australia

⁴ Geography, Planning, Spatial Sciences, University of Tasmania, Sandy Bay, TAS 7005, Australia

⁵ Ocean and Climate Physics, Lamont- Doherty Earth Observatory, Columbia University, New York, NY, USA

⁶ NASA Goddard Institute for Space Studies, New York, NY, USA

⁷ Division of Research, University of Technology Sydney, Sydney, NSW 2007, Australia

⁸ School of Ecosystem and Forest Sciences, University of Melbourne, Richmond, VIC 3121, Australia